

Accuracy Evaluation of Doppler Velocity on a Spaceborne Weather Radar through a Random Signal Simulation

SATORU KOBAYASHI, HIROSHI KUMAGAI, AND TOSHIO IGUCHI

Communications Research Laboratory, Koganei, Tokyo, Japan

5 April 2002 and 28 August 2002

ABSTRACT

Digitized signals for a spaceborne weather radar are generated to inspect a Doppler signal processor, in which the digital signals are converted to analog through an arbitrary wave generator. A conventional Rice harmonic analysis is applied to include fluctuations of Fourier coefficients explicitly in a time series rather than in an ensemble. The accuracy of Doppler velocity is studied through this simulation for a mean estimator of contiguous pulse-pair operation in a space mission, characterized by a low signal-to-noise ratio (SNR) and a short coherence time. A linear perturbation formula is shown to deviate from the simulation as the SNR decreases and the pulse-pair interval increases. Furthermore, a theoretical limit in measurement accuracy is derived, beyond which the correlation signal is to be practically regarded as white noise, losing the physical meaning of measurement.

1. Introduction

The feasibility of spaceborne weather Doppler radars has been conceptually studied by Meneghini and Kozi (1990) and Amayenc et al. (1993), who discuss both the pulse-pair method based on covariance function and the digital Fourier transform (DFT) method. In view of optimal estimators, the former method should be avoided because its variance of mean frequency is far from the Cramer–Rao bound for a broad spectrum and a long sampling interval, especially for a high signal-to-noise ratio (SNR) as described by Zrnić (1979a) and Dias and Leitao (2000). However, for a space mission, this method has been considered to be best for the following reasons: First, compact implementation in a satellite requires simple complexity of signal processing. Second, the pulse-pair method is of higher potential than the DFT method for $\text{SNR} < 0$ dBZ, typically measured during a space mission. Furthermore, for such a low SNR, the variance of mean frequency (velocity) is not as far from the Cramer–Rao bound as it is for high SNR (Doviak and Zrnić 1993; Zrnić 1979a). Based on these advantages, a practical design of a spaceborne cloud profiling radar was proposed by the European Space Agency as a part of the Earth, Clouds, Aerosols and Radiation Explorer (EarthCARE) mission (Harris and Battrock 2001). In this mission, the fairing sizes of avail-

able launchers confine the diameter of a radar antenna to 2.5 m, which will give a coherence time of $T_c \approx 100 \mu\text{s}$ at a supposed altitude of around 450 km from the earth's surface. Kobayashi et al. (2002), independently from the EarthCARE, studied pulse-pair operations from space on the basis of a linear perturbation theory. It concluded that a promising operation in regard to accuracy is a polarization diversity method (Doviak and Sirmans 1973), with a pulse-pair interval of $T_s = 60 \mu\text{s}$ and a pulse repetition interval of $T_{\text{pri}} = 222 \mu\text{s}$ (4.5 kHz). However, in this mode of operation the second signal of paired pulses coming back from the altitude of 9 km suffers from strong interference due to the ground clutter of the preceding first pulse. This is an adverse effect since one purpose of Doppler mode of operation in the EarthCARE mission is detection of cirrus existing over the altitude of 8 km. A substitute mode of operation is adoption of contiguous pulse-pair operation with $T_s = T_{\text{pri}} = 100\text{--}125 \mu\text{s}$, sacrificing the unambiguous range and the precise correction against a misaligned beam. It is, however, noted in this mode of operation that the pulse-pair interval $T_s = 100\text{--}125 \mu\text{s}$ larger than the coherence time $T_c \approx 100 \mu\text{s}$ along with low SNR (≤ 0 dB) may cause large scatters about an estimated mean value, in some cases, breaking the linearity of the perturbation theory based on small scatters about the mean value (Zrnić 1977). Thus, the validity of the perturbation theory must be confirmed through numerical simulation for the critical regime defined by $T_s \geq T_c$, and $\text{SNR} \leq 0$ dB, prior to implementation.

Corresponding author address: Hiroshi Kumagai, Communication Research Laboratory, 4-2-1 Nukii-kita Koganei, Tokyo, Japan.
E-mail: kumagai@crl.go.jp

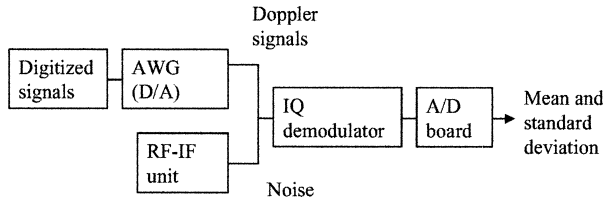


FIG. 1. A block diagram of a pulse-pair signal processor. Digitized simulated signals are converted to analog by an arbitrary waveform generator (AWG). Noise generated in an RF-IF unit merges with the signals from the AWG.

For this purpose, two kinds of numerical simulations can be considered, one of which is particle simulation, and the other is random signal simulation. Taneli et al. (2001) recently took the former simulation for a space mission along with the moderate regime defined by $T_s < T_c$ and $\text{SNR} \geq 0$, rather than the critical regime. Their results showed that the perturbation theory gave good agreement with the particle simulation for their concerned region. The random signal simulation, on the other side, has been performed mainly for ground-based parameters by a number of authors (e.g., Sirmans and Bumgarner 1975; Zrnić 1979a,b; and Dias and Leitao 2000). Advantages in this simulation are its short calculation time and easy handling of parameters such as spectral width of Doppler velocity σ_v , or coherence time T_c , and pulse-pair interval T_s .

The Communications Research Laboratory (CRL) in Japan is fabricating a pulse-pair signal processor to evaluate the feasibility of spaceborne Doppler radars. A block diagram of the processor is depicted in Fig. 1, in which digitized signals are input to an arbitrary waveform generator (AWG) to convert the signals to analog. Thereafter, noise generated in a radio frequency (RF)-intermediate frequency (IF) unit merges with the signals from the AWG, being in-phase and quadrature (IQ)-demodulated. Finally, the demodulated IQ signals enter an analog-to-digital (A/D) board to calculate the mean Doppler velocity and standard deviation for a given mean estimator. In order to operate this processor in real time, it is necessary to develop a prompt generator of simulated signals. Furthermore, these signals should be as close to real signals as possible. Experiments with this processor will be reported separately in the future. In this paper, a generation of random signals will be proposed so that the characteristic of contiguous pulse-pair operation during a space mission is well reflected. Thereafter the accuracy of Doppler velocity in a mean estimator will be evaluated through the simulation.

2. Random signal generation

Random signals on contiguous pulse-pair Doppler operation have been simulated using a harmonic analysis, referred to as the Rice method (Rice 1944), in the works of Sirmans and Bumgarner (1975) and Zrnić (1975, 1979a,b). The Rice method is presented as follows. To

a given power spectrum $S(\omega)$, the complex current $J(t)$ (voltage) at a time $t \in [0, T]$ for IQ detection can be represented in terms of a discrete Fourier series:

$$J(t) = \sum_{n=-\infty}^{\infty} c_n e^{i\omega_n t}, \quad (1)$$

in which ω_n has been defined as

$$\omega_n = 2\pi n T^{-1},$$

and the complex coefficient c_n is decomposed to the real coefficients a_n and b_n as

$$c_n = a_n - ib_n. \quad (2)$$

Here a_n and b_n are Gaussian random variables satisfying the following relations:

$$\langle a_n \rangle = \langle b_n \rangle = 0, \quad (3)$$

$$\langle a_m b_n \rangle = 0, \quad (4)$$

$$\langle a_m a_n \rangle = \langle b_m b_n \rangle = \delta_{nm} \sigma_n^2. \quad (5)$$

In these equations, $\langle x \rangle$ represents the mean value of x , and δ_{nm} designates the Cronecker delta. In short, Eqs. (3)–(5) can be summarized as

$$\langle c_m^* c_n \rangle = 2\delta_{nm} \sigma_n^2. \quad (6)$$

In these equations, σ_n^2 is related to the power spectrum $S(\omega)$ of the signal through

$$\sigma_n^2 = 2^{-1} S(\omega) \Delta \omega, \quad (7)$$

in which $\Delta \omega = 2\pi T^{-1}$ is an sampling interval of discrete frequency.

Sirmans and Bumgarner (1975) assumed the phase of c_n (i.e., $\arg c_n$) as a random variable, while fixing the amplitude of c_n at a constant defined in Eq. (8) for each frequency component n within a train of signals:

$$c_m^* c_n = 2\delta_{nm} \sigma_n^2 \text{ [c.f. Eq. (6)].} \quad (8)$$

On the other hand, Zrnić (1975) assumed an exponential distribution to $|c_n|^2$, which can be shown to be equivalent to the Rice method defined in Eqs. (1)–(7). Relating to these previous works, the following is to be mentioned: Suppose that the accuracy of a Doppler mean estimator is represented as a function of the power spectrum or its correlation function as illustrated in section 6.4-5 of Doviak and Zrnić (1993); then, as far as the same power spectrum is used, both the simulations can be proven to give the same accuracies despite the qualitative difference in random signals.

However, for inspection of the IQ signal processor, similarity of simulated signals to the experimental is substantial. We should note for the Rice method that both the amplitude and phase of c_n are fixed for a given n within a time train of T , and the distribution of c_n never fluctuates within T . Instead, the randomness and fluctuation of c_n is introduced by considering an ensemble of such trains to give the required power spectrum. Consequently, even though the original Rice method

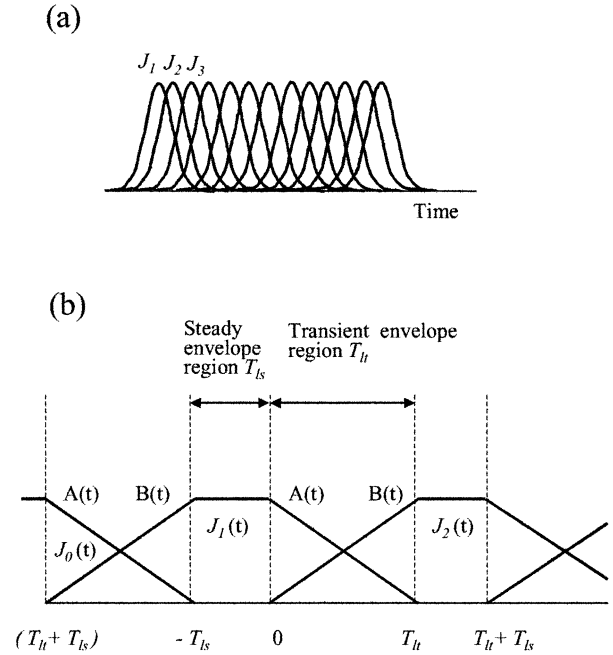


FIG. 2. Schematic diagrams of envelope functions. (a) A set of random signals $J_i(t)$ is generated independently by the Rice method. These $J_i(t)$ are connected through Gaussian-like envelope functions to give the fluctuation of the complex coefficient c_n explicitly in a time series. (b) A simplified model. Trapezoidal envelope functions, which are constituted of the steady envelope regions and the transient envelope regions, are adopted.

suffices for simulating the accuracy of velocity for the Doppler mean estimator mentioned above, the fluctuation of c_n had better be included explicitly in a time series, for which the following method can be considered.

First, a set of currents $J_i(t)$ ($i = 1, 2, \dots$) is generated independently by the Rice method. Second, these $J_i(t)$ are connected smoothly through Gaussian-like envelope functions along with mutual overlaps, as ideally shown in Fig. 2a. However, simulating this model consumes a lot of time due to a large number of currents $J_i(t)$. To simplify the problem, Fig. 2b shall be considered in place of Fig. 2a. In the concerned time region, three random currents, $J_0(t)$, $J_1(t)$, and $J_2(t)$, are generated from a power spectrum $S(\omega)$, and trapezoidal envelope functions instead of the Gaussian-like are introduced, being constituted of two parts: transient envelope regions of time duration T_{tr} extending in $[-(T_{tr} + T_{st}), -T_{st}]$ and $[0, T_{tr}]$, and the steady envelope regions in between. In the first transient region $[-(T_{tr} + T_{st}), -T_{st}]$, the random signal $J_1(t)$ starts growing with an envelope function $B(t)$ and reaches the constant amplitude of unity, holding in the steady region $[-T_{st}, 0]$. In the second transient region $[0, T_{tr}]$, the signal $J_1(t)$ decays with an envelope function $A(t)$, and, instead, the other random signal $J_2(t)$ grows again with the envelope function $B(t)$. For macroscopically homogeneous clouds, we can assume that the $\langle J^*(t_1)J(t_2) \rangle$ is determined uniquely by

the correlation function $r(t)$ corresponding to a power spectrum $S(\omega)$ during a radar scan, namely

$$\langle J^*(t_1)J(t_2) \rangle = r(t_2 - t_1) \quad (9)$$

for arbitrary t_2 and t_1 within a radar scan. In the steady region, Eq. (9) is automatically satisfied. In the transient region $[0, T_{tr}]$, the total signal can be written in the form

$$J(t) = A(t)J_1(t) + B(t)J_2(t), \quad (10)$$

and the time correlation can be represented as

$$\langle J^*(t_1)J(t_2) \rangle = [A(t_1)A(t_2) + B(t_1)B(t_2)]r(t_2 - t_1). \quad (11)$$

However, Eq. (9) indicates that the functions $A(t)$ and $B(t)$ must satisfy

$$[A(t_1)A(t_2) + B(t_1)B(t_2)] = 1. \quad (12)$$

Trivially, rigorous solutions of $A(t)$ and $B(t)$ cannot exist except for constants. Thus, Eq. (12) should be assumed to be nearly equal to unity as an approximation. Furthermore, simple forms are assumed as follows:

$$A(t) = \begin{cases} 1 & t < 0 \\ \sqrt{1 - (t/T_{tr})^2} \text{ or } \cos\left(\frac{T_{tr}}{2r}t\right) & t \in [0, T_{tr}] \\ 0 & t > T_{tr}, \end{cases}$$

$$B(t) = \begin{cases} 0 & t < 0 \\ t/T_{tr} \text{ or } \sin\left(\frac{T_{tr}}{2r}t\right) & t \in [0, T_{tr}] \\ 1 & t > T_{tr}. \end{cases} \quad (13)$$

In order to calculate Eq. (12), the time t_2 is set at

$$t_2 = t_1 + T_s, \quad (14)$$

in which T_s designates a pulse-pair interval. Then Eq. (12) can be written as a function of the first pulse time t_1 along with the parameters T_s , T_{tr} , and T_{st} :

$$f(t_1; T_s, T_{tr}, T_{st}) = [A(t_1)A(t_1 + T_s) + B(t_1)B(t_1 + T_s)] \approx 1. \quad (15)$$

Since the transition duration T_{tr} and the steady duration T_{st} are parameters within which signal correlation must hold, we can consider that these parameters are at least the length of coherence time T_c . In this paper, the steady duration T_{st} is assumed to be $T_{st} = 2T_c \approx 200 \mu\text{s}$ so that we can continuously evaluate the accuracy beyond the pulse interval $T_s \approx 120 \mu\text{s}$, as required in the EarthCARE mission. Furthermore, from numerical calculations for Eq. (15), the transient durations of $T_{tr} = 2T_c$ and $T_{tr} = 10T_c$ are found to be adopted as a good parameter up to $T_s \approx 50 \mu\text{s}$ and $T_s \approx 160 \mu\text{s}$, respectively.

3. Accuracy of Doppler velocity in a space mission

The evaluation of accuracy in Doppler velocity is performed for contiguous pulse-pair operation. Suppose

that a radar antenna of 2.5-m diameter with a beamwidth of 0.089° aims toward the nadir direction from a platform moving at an altitude of 450 km at the velocity of $v_{pl} = 7.64 \text{ km s}^{-1}$, then the total spectral width of Doppler velocity can be considered to be decomposed (Kobayashi 2002; Kobayashi et al. 2002):

$$\sigma_v^2 = \sigma_{dop}^2 + \sigma_{cld}^2 + \sigma_{win}^2. \quad (16)$$

In Eq. (16), σ_{cld} and σ_{win} designate the spectral widths due to the distributions of cloud falling velocity weighted by backscattering cross sections and wind velocity, respectively, which are assumed to be $\sigma_{cld} = 0.5 \text{ m s}^{-1}$ (Gossard et al. 1997) and $\sigma_{win} = 1 \text{ m s}^{-1}$ (Amayenc et al. 1993). The σ_{dop} denotes the spectral width reflecting the combined effect of Doppler fading and vertical wind shears (Kobayashi 2002). Ignoring the wind shears, we can calculate $\sigma_{dop} = 3.72 \text{ m s}^{-1}$. Hence Eq. (16) yields the total velocity width of $\sigma_v = 3.85 \text{ m s}^{-1}$, and the corresponding coherence time is given by

$$T_c = (\sqrt{2}k\sigma_v)^{-1} \approx 93 \mu\text{s}, \quad (17)$$

where k is the radiation wavenumber for 95.04 GHz. Converting the spectral width of Doppler velocity to the frequency width through the equation $\sigma_\omega = 2k\sigma_v$, the IQ current $J(t)$ can be simulated as in section 2. A mean estimator over an along-track integration of distance d is presented for contiguous pulse pairs in the form (Zrnić 1977)

$$R(T_s) = N^{-1} \sum_{i=0}^{N-1} J^*[iT_s]J[(i+1)T_s], \quad (18)$$

in which N designates the total number of pulse pairs in the distance d with the platform velocity v_{pl} , given by

$$N = d/(v_{pl}T_s). \quad (19)$$

Finally, the estimated mean Doppler velocity is derived from

$$\bar{v} = (2kT_s)^{-1} \arg R(T_s), \quad (20)$$

and the standard deviation (accuracy) of \bar{v} , referred to as std dev (\bar{v}), can be calculated through iterations of the simulation.

Simulation results of std dev (\bar{v}) for $d = 1 \text{ km}$, which is required by the EarthCARE mission (Harris and Batrick 2001), are plotted in Fig. 3 for the parameters $T_{it} = 10T_c$ and $T_{is} = 2T_c$. The ordinate and abscissa represent the std dev (\bar{v}) and the pulse-pair interval T_s , respectively. The solid lines are generated from the averages of 10 000 iterations for the SNRs from -15 to $+10 \text{ dB}$, on which the superimposed noises have been assumed to be white. The broken lines are calculated by a perturbation formula in Doviak and Zrnić (1993). Good agreements are seen for $T_s \lesssim 130 \mu\text{s}$ with higher SNRs, as expected from the postulation of the perturbation theory. In addition, simulations for the other parameters, $T_{it} = 2T_c$ and $T_{is} = 2T_c$, were also performed, the result of which was almost identical to that shown

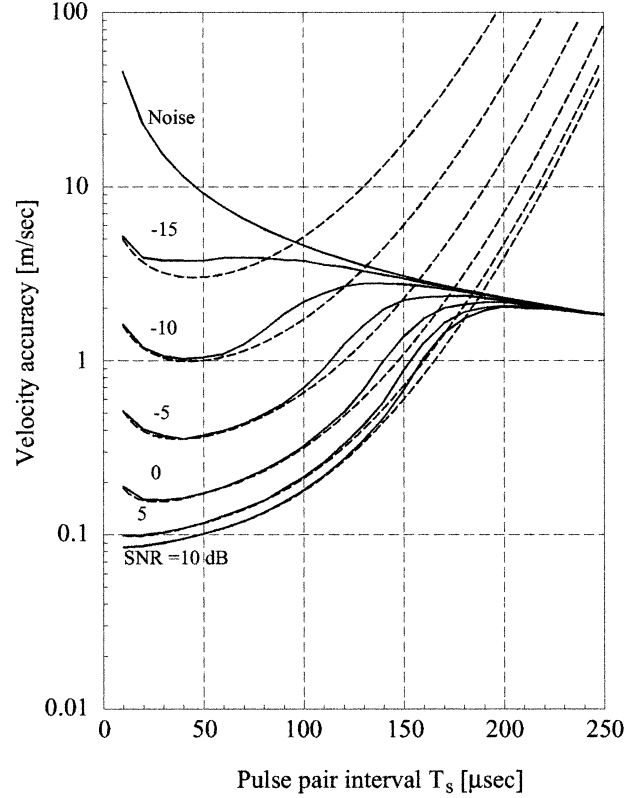


FIG. 3. Accuracy in Doppler velocity vs pulse-pair interval T_s for contiguous pulse-pair operation. The along-track integration and the spectral width of velocity are set at $d = 1 \text{ km}$ and $\sigma_v = 3.85 \text{ m s}^{-1}$ ($T_c = 93 \mu\text{s}$), respectively. The simulations are performed over 10 000 times, as described in section 2, for the parameters $T_{it} = 10T_c$ and $T_{is} = 2T_c$. The noises superimposed on the data SNR = -15 to $+10 \text{ dB}$ have been assumed to be white. The broken lines are calculated by a perturbation formula of Doviak and Zrnić (1993).

in Fig. 3; for $T_s < 50 \mu\text{s}$, especially, the agreement was excellent.

Notice that all the solid lines in Fig. 3 converge to the line marked “Noise” in the region of $T_s > 200 \mu\text{s}$, which can be explained as follows. As the SNR decreases and T_s increases, the Doppler correlation signal is expected to behave like white noise. The ensemble average of \bar{v} , referred to as $\langle \bar{v} \rangle$, cannot be uniquely defined rigorously for white noise, because the value of $\langle \bar{v} \rangle$ strongly fluctuates from one ensemble to another. In such a situation, however, once $\langle \bar{v} \rangle$ is determined for a given ensemble, which is always possible, std dev (\bar{v}) can be formally calculated as shown below. Without losing generality, we can assume $\langle \bar{v} \rangle = 0$, or equivalently $\langle \bar{\theta} \rangle = 0$, along with the phase $\bar{\theta} = \arg R(T_s)$ in the IQ space. Then $\bar{\theta}$ distributes uniformly in $[-\pi, \pi]$ for the white noise, and the standard deviation of $\bar{\theta}$ can be calculated:

$$\text{std dev}(\bar{\theta}) = 3^{-0.5} \pi. \quad (21)$$

We thus obtain the expression of the Noise line as

$$\text{std dev}(\bar{v}) = \text{std dev}(\bar{\theta})/2kT_s \approx 460T_s^{-1}(\mu\text{s}). \quad (22)$$

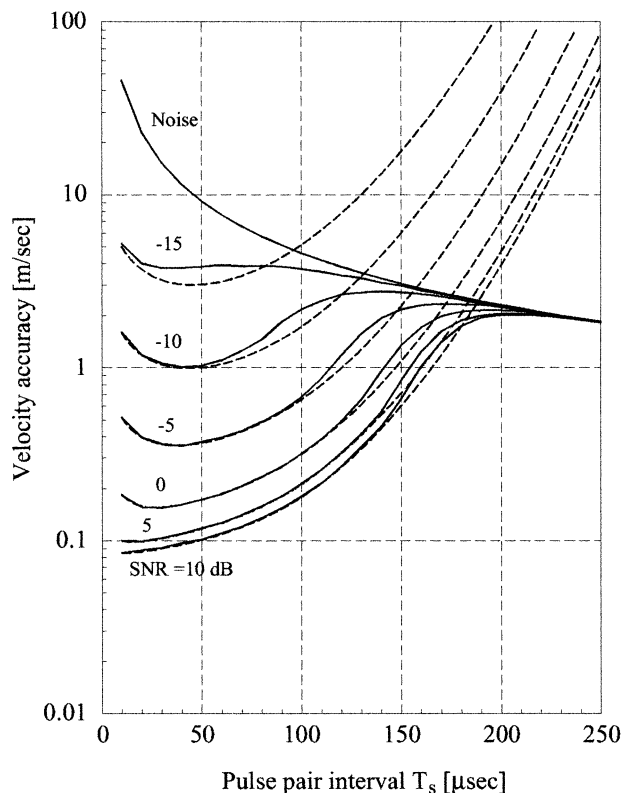


FIG. 4. Accuracy in Doppler velocity vs pulse-pair interval T_s for contiguous pulse-pair operation. The simulations, performed by the original Rice method, are otherwise the same as in Fig. 3. Good agreement with Fig. 3 indicates that the method of this paper (Fig. 3) gives the same correlation and power spectrum as the original Rice method, despite a qualitative difference in random signals.

This Noise line indicates that accuracies near it have little physical meaning in view of measurements.

4. Conclusions and discussion

Signals for a spaceborne weather radar have been simulated as discussed in section 2. This simulation reflects the fluctuation of the complex coefficient c_n explicitly in a time series (i.e., during a radar scan), which, on the other hand, appears in an ensemble in the original Rice method. This feature of the former method suits for the experiment of Fig. 1, because the real-time processing for the fluctuating signal is substantial. However, it is noted that for the parameters satisfying Eq. (15), such as $T_{lt} = 10T_c$ and $T_{ls} = 2T_c$, the method in this paper gives the same time correlation and power spectrum as the original Rice method does. Thus, as far as the accuracy of the mean estimator of Eq. (18) is concerned, both the methods should give identical results. In fact, the simulation of Fig. 3 showed excellent agreement with that of the original Rice method as shown in Fig. 4.

In Figs. 3 and 4 the emphasis is placed on deviations from the perturbation theory on low SNRs (≤ 0 dB) and/

or T_s longer than a coherence time $T_c = 93 \mu\text{s}$. Especially at $T'_s \approx 150 \mu\text{s}$ large deviations occur even for relatively high SNRs (5 and 10 dB), because the signals lose the coherence, approaching noise. Obviously, monotonously increasing degradations of the accuracy on the perturbation theory with increasing T_s and decreasing SNR, seen in Figs. 3 and 4, are unrealistic, but they should be suppressed by nonlinear effect, as the simulation results show. This nonlinearity can also be expected from the following consideration. Suppose that an ensemble of $R(T_s)$, defined in Eq. (18), has scatters of ΔI and ΔQ in the IQ space about a mean value of $\langle \text{Re}R(T_s) \rangle = I_{\text{me}}$, and $\langle \text{Im}R(T_s) \rangle = 0$, that is, $\langle \bar{\theta} \rangle = 0$. Since it is intractable to know the exact expression of std dev $\langle \bar{\theta} \rangle$, we can roughly represent as

$$\text{std dev}(\bar{\theta}) \approx \arctan(\Delta Q/I_{\text{me}}), \quad (23)$$

which can be linearized for $|\Delta Q| \ll 1$:

$$\text{std dev}(\bar{\theta}) \approx \Delta Q/I_{\text{me}}. \quad (24)$$

Equation (24) is related to the perturbation theory in previous works, and is also the origin of the divergence for $\Delta Q/I_{\text{me}} \rightarrow \infty$ as $T_s \rightarrow \infty$. On the other hand, the nonlinear expression Eq. (23) will never diverge, as $\Delta Q/I_{\text{me}} \rightarrow \infty$. Here the exact asymptotic form of std dev $\langle \bar{\theta} \rangle$ in a large T_s is again unknown, but the form in the extreme limit of large T_s has been already given exactly in Eq. (21). Additionally, it should be mentioned that the degradation of velocity accuracy with short $T_s \approx 10 \mu\text{s}$ is caused by reduction in phase resolution for the small T_s but not related to increase in the value of std dev $\langle \bar{\theta} \rangle$ (Kobayashi et al. 2002).

The EarthCARE (Harris and Battrick 2001) requires Doppler measurement to an accuracy of 1 m s^{-1} over an along-track integration of 1 km for clouds of -20 dBZ, corresponding to $\text{SNR} = -5$ dB under the parameters of this paper. Our simulations indicate that this requirement can be achieved for $T_s \approx 120 \mu\text{s}$ around which the perturbation theory is effective with a little deviation from the values of simulations, as shown in Figs. 3 and 4, thus also supporting linear analyses in Kobayashi et al. (2002).

Throughout this paper, the superimposed noises have been assumed to be white. However, when short $T_s \approx 10 \mu\text{s}$ is concerned, this assumption cannot always be guaranteed, as in the hardware experiment in Fig. 1; therefore, colored noise, which may have significant impact should be taken into account.

REFERENCES

- Amayenc, P., J. Testud, and M. Marzoug, 1993: Proposal for a spaceborne dual-beam rain radar with Doppler capability. *J. Atmos. Oceanic Technol.*, **10**, 262–276.
- Dias, J. M. B., and J. M. N. Leita, 2000: Nonparametric estimation of mean Doppler and spectral width. *IEEE Trans. Geosci. Remote Sens.*, **38**, 271–282.
- Doviak, R. J., and D. Sirmans, 1973: Doppler radar with polarization diversity. *J. Atmos. Sci.*, **30**, 737–738.

- , and D. S. Zrnić, 1993: *Doppler Radar and Weather Observations*. 2d ed. Academic Press, 562 pp.
- Gossard, E. E., J. B. Snider, E. E. Clothiaux, B. Martner, J. S. Gibson, R. A. Kropfli, and A. S. Frisch, 1997: The potential of 8-mm radars for remotely sensing cloud drop size distributions. *J. Atmos. Oceanic Technol.*, **14**, 76–87.
- Harris, R. A., and B. Battrick, Eds., 2001: *EarthCARE—Earth, Clouds, Aerosols and Radiation Explorer*. ESA Publications Division, 130 pp.
- Kobayashi, S., 2002: A unified formalism of incoherent, quasi-coherent, and coherent correlation signals on pulse-pair Doppler operation for a cloud-profiling radar: Aiming for a space mission. *J. Atmos. Oceanic Technol.*, **19**, 443–456.
- , H. Kumagai, and H. Kuroiwa, 2002: A proposal of pulse-pair operation on a spaceborne cloud-profiling radar in the W band. *J. Atmos. Oceanic Technol.*, **19**, 1294–1306.
- Meneghini, R., and T. Kozu, 1990: *Spaceborne Weather Radar*. Artech House, 199 pp.
- Rice, S. O., 1944: Mathematical analysis of random noise. *Bell Syst. Tech. J.*, **23**, 282–332.
- Sirmans, D., and B. Bumgarner, 1975: Numerical comparison of five mean frequency estimators. *J. Appl. Meteor.*, **14**, 991–1003.
- Taneli, S., E. Im, S. L. Durden, L. Facheris, D. Giuli, Z. S. Haddad, and E. A. Smith, 2001: Spaceborne radar measurements of vertical rainfall velocity: The non-uniform beam filling considerations. *Proc. 2001 Int. Geoscience and Remote Sensing Symp.*, Vol. II, Sydney, Australia, IEEE, 679–681.
- Zrnić, D. S., 1975: Simulation of weatherlike Doppler spectra and signals. *J. Appl. Meteor.*, **14**, 619–620.
- , 1977: Spectral moment estimates from correlated pulse pairs. *IEEE Trans. Aerosp. Electron. Syst.*, **AES-13**, 344–354.
- , 1979a: Estimation of spectral moment for weather echoes. *IEEE Trans. Geosci. Electron.*, **GE-17**, 113–128.
- , 1979b: Spectrum width estimates for weather echoes. *IEEE Trans. Aerosp. Electron. Syst.*, **AES-15**, 613–619.